Electron Photoejection from Corannulene Dianion and Li^+-Mediated Recombination of the Photogenerated Species

Roy Shenhar,[†] Itamar Willner,*[,†] Dorin V. Preda,[‡] Lawrence T. Scott,[‡] and Mordecai Rabinovitz*[,†,§]

Department of Organic Chemistry, The Hebrew University of Jerusalem, Jerusalem, Israel 91904, and Department of Chemistry, Boston College, Chestnut Hill, Massachusetts 02467-3860

Received: June 30, 2000

The antiaromatic corannulene dianion, Cor^{2-}, undergoes photoejection of an electron to yield an intimate cage complex of $Cor^{\bullet-}$ and the electron. Part of the complex species undergoes cage recombination, $k_{rec}^1 = 1.1 \times 10^6\ s^{-1}$, while the other part of complex separates, $k_s = 2.3 \times 10^6\ s^{-1}$, and yields $Cor^{\bullet-}$ and a Li^+/e^- ion pair. Diffusional recombination of the later products proceeds with a bimolecular rate constant corresponding to $k_{rec}^2 = 1.3 \times 10^9\ M^{-1}\ s^{-1}$. Time-resolved laser flash-photolysis and FT-EPR experiments are used to characterize the transient species.

Introduction

Anions of organic molecules are able to serve as electron donors due to the occupation of high-lying orbitals in the π-system, i.e. the LUMO of the neutral compound. Irradiation of a solution of in situ generated polycyclic aromatic carbanions often results in electron ejection.[1−10] Whereas photoejection of an electron from a neutral compound generates oppositely charged redox species that attract each other, resulting in fast back electron transfer, light induced electron ejection from polyanionic species results in photoproducts that repel each other, and hence their recombination is retarded. That is, the electrostatic repulsion of the species introduces a barrier that stabilizes the photoproducts against recombination. An interesting application of this feature is photogalvanic cells.[11]

Experiments on electron photoejection from carbanions have been performed for several decades. Hoijtink et al. illuminated polycyclic aromatic carbanions in frozen solutions of 2-methyltetrahydrofuran (2-MTHF) and observed the photoejected electron at its characteristic absorbance in the near-IR region[12−14] as well as the EPR of the photoejected electron.[13] The rigidity of the solvent prevented the back reaction, but softening of the glass (by heating from 77 K to 98 K) enabled the electron to diffuse back to regenerate the original anion.[13,14] The back reaction in the rigid medium could also be facilitated by irradiating the photogenerated electron in the IR region (energy which is lower than the energy required for the photooxidation of the original anion).[13] Using these methods, it was deduced that the mobility of electrons in softened glass is significantly higher than the mobility of the ionic species[14] and that the electron is caught upon ejection in cavities of the rigid solvent (rather than in cationic traps).[13] Therefore Hoijtink et al. could attribute the near-IR band and the corresponding EPR signal arising from irradiation of the rigid solution to a solvated photoelectron, bound within a solvent cage.[13] Similarly, data on the ion pairing of the alkali metal with the dianion and the radical-anion could be deduced as well.[14] Furthermore, pulse radiolysis and flash photolysis experiments have elucidated the interaction of electrons with alkali metal cations.[15,16] It was suggested that a collapse between the electron and cation to yield an atom occurs,[16] but later studies suggested the formation only of an intimate cation−electron solvated pair.[4]

CHART 1

Flash photolysis experiments on liquid solutions of aromatic anions were performed mainly by Szwarc, Fox, Giling, and others,[1−6] and these provided quantitative information on the kinetics involved with regeneration of the ground-state anion after the photoinduced electron ejection, as well as important qualitative features of the system regarding the solvation states of the species under investigation. Based on these studies it was concluded that the degree of association of the electron with the cation increases for bigger cations and at higher temperatures.[2] Giling et al. also established the path of the back reaction, which was demonstrated to proceed by a fast primary association of the electron with the cation prior to a secondary back-reaction with the complementary photogenerated neutral compound.[3−5] Since electron photoejection may also be the primary step of photodissociation, studying the kinetics of the recombination of the photoproducts provided data characterizing the electron-transfer initiation of anionic polymerization processes.[8] Other uses of the electron photoejection processes involved determination of disproportionation rate constants of a variety of radical anions.[8,17]

Corannulene (Cor), a bowl-shaped fragment of C_{60}, has been reduced in the past by different alkali metals, and a charging degree as high as a Cor tetraanion has been observed upon the reduction of Cor with some of the metals used.[18−20] The $Li^+{}_4-Cor^{4-}$ has attracted substantial interest since four negative charges are condensed in a small molecular perimeter, and since various studies indicate that $Li^+{}_4-Cor^{4-}$ exists as a supramolecular dimer in solution.[19,21]

[†] The Hebrew University of Jerusalem.
[‡] Boston College.
[§] Tel: ++972-2-6585281. Fax: ++972-2-6527547. E-mail: mordecai@vms.huji.ac.il.

10.1021/jp002344h CCC: $19.00
Published on Web 10/28/2000

Previous studies have addressed the electron photoejection from Cor tetraanion using flash photolysis and EPR measurements.[10] In those studies, however, the photophysical properties of the intermediary Cor dianion were not explored, although several fundamental features of the dianion suggest that the photoinduced electron ejection from these polyanions could also be of basic interest. The Cor dianion is an intriguing species: it is relatively stable species even though it is considered to be antiaromatic (22πe, presumably arranged as an inner 6-electron aromatic cyclopentadienyl anion surrounded by a 16-electron antiaromatic 15-annulenyl anion). The π-system is still curved, although the bowl-to-bowl inversion barrier ($\Delta G_{230}^{\ddagger} = 8.8$ kcal/mol)[22] is somewhat reduced relative to that of the neutral hydrocarbon ($\Delta G_{209}^{\ddagger} = 10.2$ kcal/mol),[23] as determined from measurements on the potassium salt of an alkyl substituted derivative.[22] The ^{1}H NMR spectrum of the Cor dianion acquired at a low temperature shows a broad absorption at δ −5.6 ppm. This inordinately high field chemical shift reflects the antiaromatic character, and the exceptionally broad width of the peak implies a close, low-lying triplet state. Calculations have shown that the lowest unoccupied molecular orbital (LUMO) of Cor is doubly degenerate, which supports the last assumption.[18]

Here we wish to report on the photoinduced electron ejection from the curved, anti-aromatic Cor dianion, the kinetics of recombination of the photoejected electron with the radical-anion, and the spectroscopic features of Cor anions.

Experimental Section

The Determination of Extinction Coefficients of Corannulene Anions. A glass apparatus was assembled to allow the accurate determination of the spectroscopic features of the respective anions under inert conditions. This apparatus, shown in Figure 1, consists of an ampule, a closed buret and a 1-mm optical path quartz cell attached at the buret's top.

A weighted amount (within the accuracy of ±0.002 mg) of ca. 2 mg of pure Cor was inserted into the ampule. The glass apparatus was then filled with argon; a lithium wire was freshly produced and directly inserted into the ampule, and immediately afterward the apparatus was connected to a vacuum line. The whole line and the glassware were flame-dried under vacuum. Previously distilled (and dried over a sodium−potassium alloy) tetrahydrofuran (THF) was vacuum-transferred to the buret part of the glassware. Degassing was performed by the freeze−pump−thaw method, and the apparatus was then flame-sealed under less than 0.01 mbar pressure.

Upon transferring of a small amount of THF to the ampule the Cor dissolved completely, and the resulting solution was allowed to react with the lithium wire. After a short time interval the solution changed its color from faint yellow to intense green, which indicated the formation of the radical-anion. The whole apparatus was then washed with the solution in order to dry the glass from trace amounts of moisture. This was usually attended by disappearance of the green color. Transferring the solution to the ampule and concentrating it (by vacuum transfer of most of the solvent to the buret part) allowed a further contact of the solution with the metal, which regenerated the radical-anion.

After the green color persisted in the solution upon the repeated treatment of the Cor solution as described, the reduction of the sample was performed with a fixed volume of the solvent in order to maintain a constant concentration of the anionic species through the experiment. To determine the accurate point in time at which most of the Cor has been converted to its

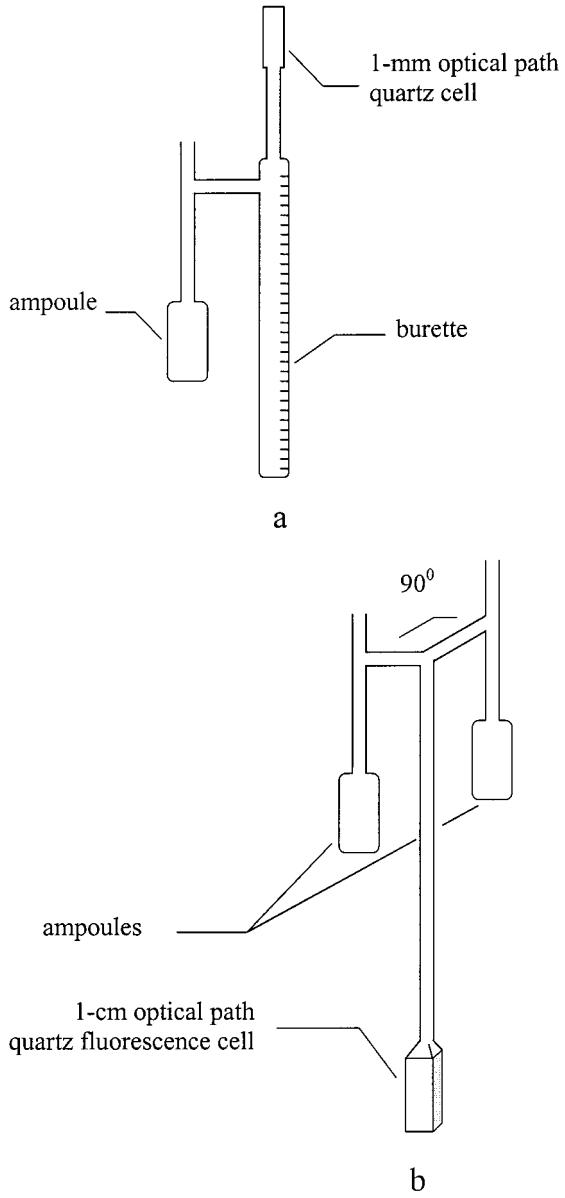

Figure 1. Glassware assembly fabricated for: (a) The determination of the absorbance spectra of the respective anions. (b) The preparation of samples for the kinetic analysis of the electron photoejection.

radical-anion, the UV−Vis spectrum of the solution was measured several times through the course of reduction. Plotting the OD at λ_{max} of the radical-anion against time yielded a curve exhibiting a maximum OD value. This value was taken to correspond approximately to the complete transformation of the neutral Cor to Cor radical-anion.

The same method was applied for the determination of the absorbance features of the Cor dianion (purple solution) and the tetraanion (brown solution) of Cor, assuming that each maximum is indeed indicative of an almost complete transformation from one reduction state to the next. This assumption is based on complementary NMR and EPR experiments, which reveal that when the dianion is visible there is no neutral compound and no radical-anion (which for even minute amounts of the latter would have extinguished the NMR peaks of the dianion). NMR also shows that after a few days of continuous reduction only tetraanion peaks are visible.[20]

Kinetic Measurements. *Glassware.* The glassware that was fabricated for the kinetics measurements had to satisfy the following two constraints:

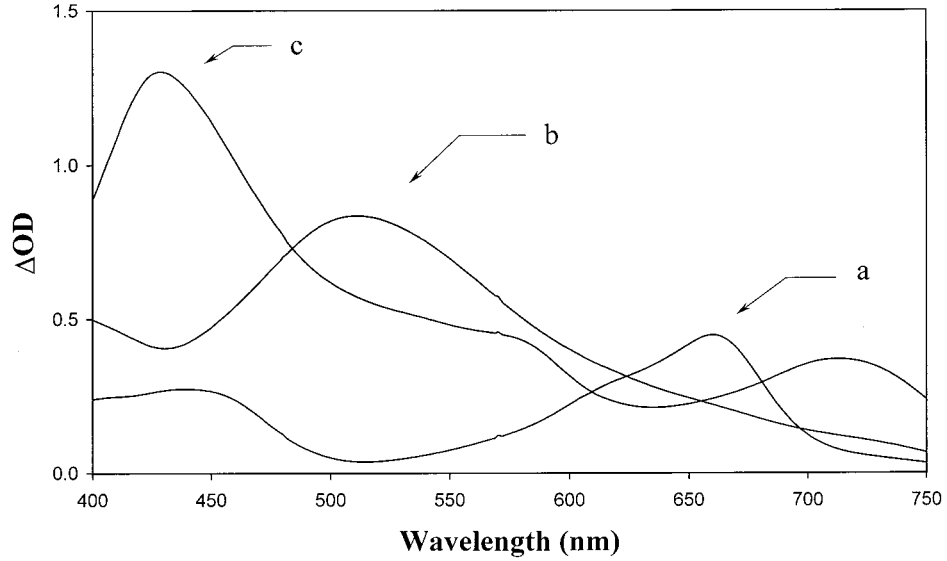

Figure 2. Steady state UV−Vis spectra of the charged species derived from corannulene: (a) radical anion, (b) dianion, (c) tetraanion.

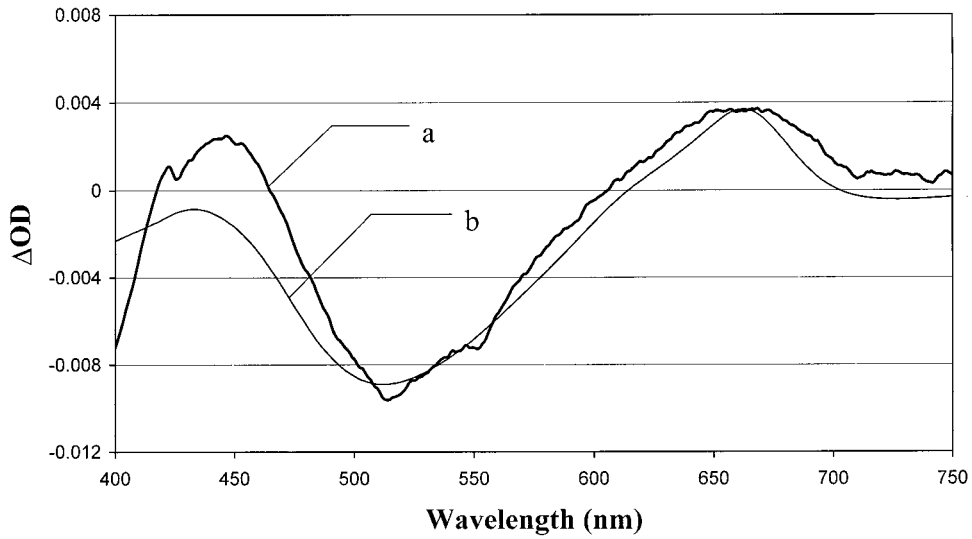

Figure 3. (a) Transient UV−Vis spectrum of the irradiated of Cor dianion solution (excitation at $\lambda = 512$ nm). The spectrum is acquired 100 μs after the laser pulse. The bleaching of the dianion can be observed at $\lambda = 512$ nm, and the transient formation of the radical anion is reflected as the positive ΔOD at 659 nm. (b) The curve obtained upon subtraction of the steady-state UV−Vis spectrum of the Cor^{2-} from that of the $Cor^{\bullet -}$ (normalized to the yield of the photoprocess).

(1) To initiate the reduction within a reasonable time from the first contact with the lithium wire, a fairly high concentration of the organic substance is needed. This high concentration used for charging is, however, not suitable for the optical measurement, due to the high molar extinction coefficients of the charged species. Therefore the glassware apparatus was fabricated to enable both the concentration and dilution of the sample, respectively.

(2) As the optical cell by itself is not suitable for vacuum distillation, the glass apparatus was constructed of two ampules and a 1-cm optical-path quartz fluorescence cell, as shown in Figure 1b (for the EPR experiments an EPR tube replaced the optical cell). The reduction process took place in the ampule containing the lithium wire. By transferring a small amount of the material to the optical cell and most of the solution to the vacant ampule, distillation (by vacuum transfer) of solvent to the lithium ampule, and then transferring of the distilled solvent to the optical cell enabled the generation of a dilute solution of the respective anion in the optical cell.

The UV−Vis Flash Photolysis System. A Nd:YAG laser (Continuum Surelite I), equipped with second and third harmonic crystals was used as the base light source. The 355-nm third harmonic light source (1 Hz repetition rate, ∼150 mJ/pulse, 5.5 ns pulse width) was used to pump an optical parametric oscillator (Continuum Surelite OPO), resulting in monochromatic light pulses within the visible range (300−700 nm) at a constant power output of 20−25 mJ/pulse (wavelength dependent). The excitation of the Cor dianion was performed at its absorbance maximum, $\lambda_{max} = 512$ nm, to obtain the optimal results, (nonetheless, the photoprocess also occurred when irradiating with a 532-nm beam). The excitation pulses hit the sample chamber while the analytical light source analyzed the spectral changes in the sample chamber in a perpendicular configuration.

The analytical light source for probing the absorbance changes in the sample as a result of the laser pulse excitation was a pulsed Xe arc lamp. Since the absorbance transients of some of the species were in the ms time scale, pulsing the analytical

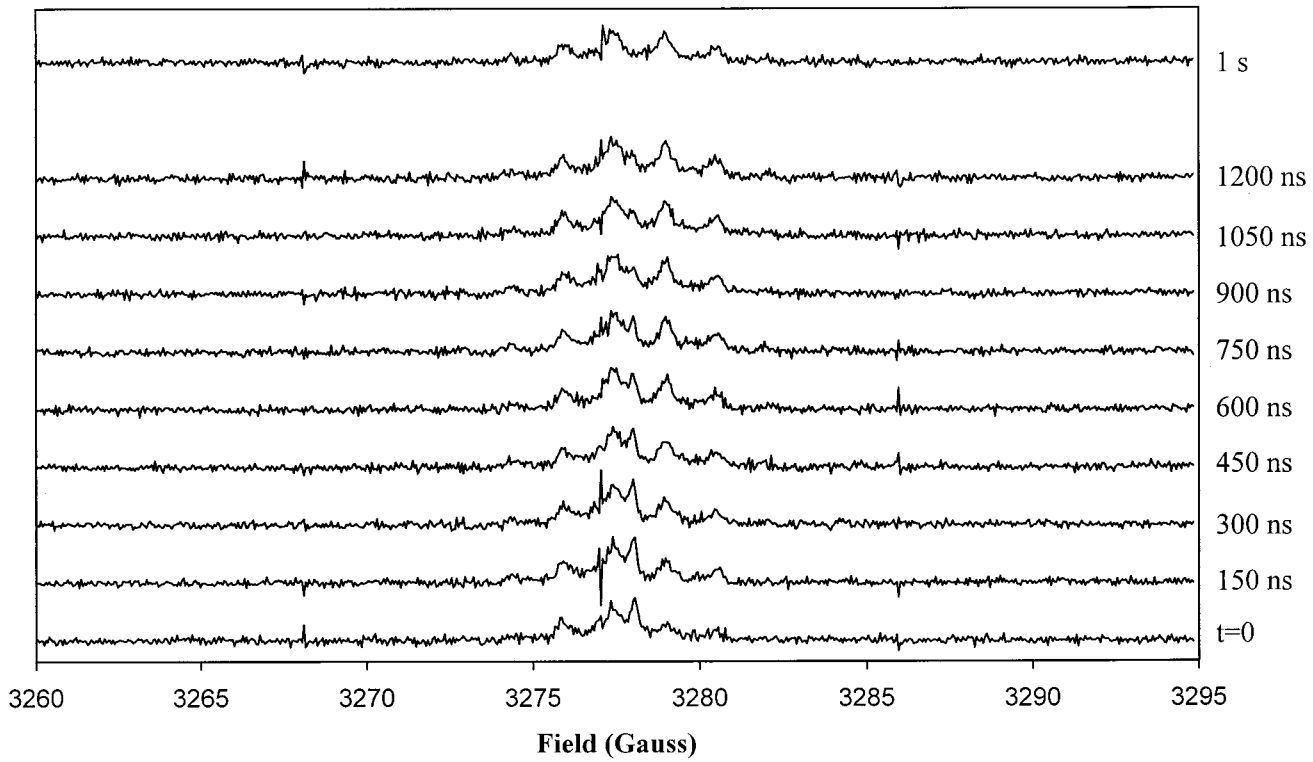

Figure 4. Transient EPR spectra of the irradiated Cor dianion solution (excitation at $\lambda = 532$ nm), acquired at selected time intervals after the laser pulse. Note the decaying signal of the photoelectron at 3278 Gauss.

lamp was applied only for probing the fast transient components. Noise reduction for the total curve was achieved by electronic amplification of the signal with a 1 kΩ resistor.

The spectral changes were recorded by two complementary detection systems, which were interchangeable by changing the position of a mirror. One detection system consists of a monochromator-photomultiplier (PMT) detection system combined with an oscilloscope (Textronix, model 2430A). This detection system was used to follow transient absorbances at a fixed wavelength. The data recorded with the oscilloscope were transferred to a personal computer for further processing and kinetic analysis. The second detection system was an intensified charge coupling device detection system (ICCD), used to acquire a transient spectrum at a certain point in time after the laser pulse. The light passing through the sample was guided through an optical fiber, projected on a 150-grooves/mm grating (Acton Spectrometer, model SP-150) and reflected on the ICCD detector. The ICCD detector (Princeton Instruments) was cooled to −30 °C in order to increase its sensitivity. A controller (Princeton Instruments, model ST-130) controlled the ICCD's temperature and the data transfer to a personal computer, and a high voltage pulse generator (Princeton Instruments, model PG-200) was used to allow for exposure duration as short as 100 ns. The PMT detection system was synchronized (LKS, Applied Photophysics) directly with the laser Q-switch. The synchronization of the ICCD detector with the laser system was achieved with the LKS system coupled to a delay generator (Stanford). Nonlinear curve fit analyses were performed using the Microcal Origin 5.0 software package.

The FT-EPR Flash Photolysis System. The irradiation source for the FT-EPR flash-photolysis system was a Nd:YAG laser (Continuum 661-2D), equipped with a second harmonic crystal. The 532 nm pulses (20 Hz repetition rate, ∼25 mJ/pulse, 12 ns pulse width) were guided with prisms to the center of the cavity of the EPR. The cavity was connected to a liquid nitrogen transfer line, which was used to cool the sample to 175 K. The detection system was a pulsed FT-EPR spectrometer (Bruker ESP 380, 24 ns microwave pulses). Free induction decay (FID) signals were detected at selected delay times after the laser pulse. The end spectrum of the Cor radical anion (ca. 1 s after photoexcitation) was used for the phase correction of the series of spectra recorded in the time domain $t = 0$ to $t = 1200$ ns.

Results and Discussion

Figure 2 shows the absorbance spectrum of the Cor radical anion, curve (a) ($\lambda_{max} = 659$ nm, $\epsilon = 6200$ M^{-1} cm^{-1}), the Cor dianion, curve (b) ($\lambda_{max} = 512$ nm, $\epsilon = 11700$ M^{-1} cm^{-1}) and the Cor tetraanion, curve (c) ($\lambda_{max} = 429$ nm, $\epsilon = 18200$ M^{-1} cm^{-1}), formed in the different phases of reduction of Cor by lithium metal. The vastly different molar extinction coefficients of Cor^{2-} and $Cor^{\bullet -}$ at 512 and 532 nm allow the selective irradiation of Cor^{2-} and spectral analysis of the photoejection process. Photoexcitation of the Cor^{2-} solution, ca. 4×10^{-5} M, $\lambda = 512$ (the parent solution does not include $Cor^{\bullet -}$ as confirmed by EPR and absorbance measurements) yields the transient spectrum shown in Figure 3, curve (a). It includes a bleached absorbance band at $\lambda = 512$ nm, consistent with the disappearance of Cor^{2-}, and the build-up of an absorbance band at $\lambda = 659$ nm, consistent with the formation of $Cor^{\bullet -}$. Analysis of the transient spectrum by the subtraction of the Cor^{2-} from $Cor^{\bullet -}$ spectrum (normalized for the yield of the photoprocess) generates a calculated spectrum that almost coincides with the experimental transient spectrum, Figure 3, curve (b).

EPR measurement at 175 K (no EPR signal could be observed at room temperature due to fast T2 relaxation times) of the solution showed no signal before the beginning of the flash-photolysis experiment. Laser excitation of the Cor^{2-} solution resulted in a time-dependent FID signal (averaging of 50 scans for each time interval), Figure 4. A close comparison of the spectra reveals two superimposed spectral patterns. The first

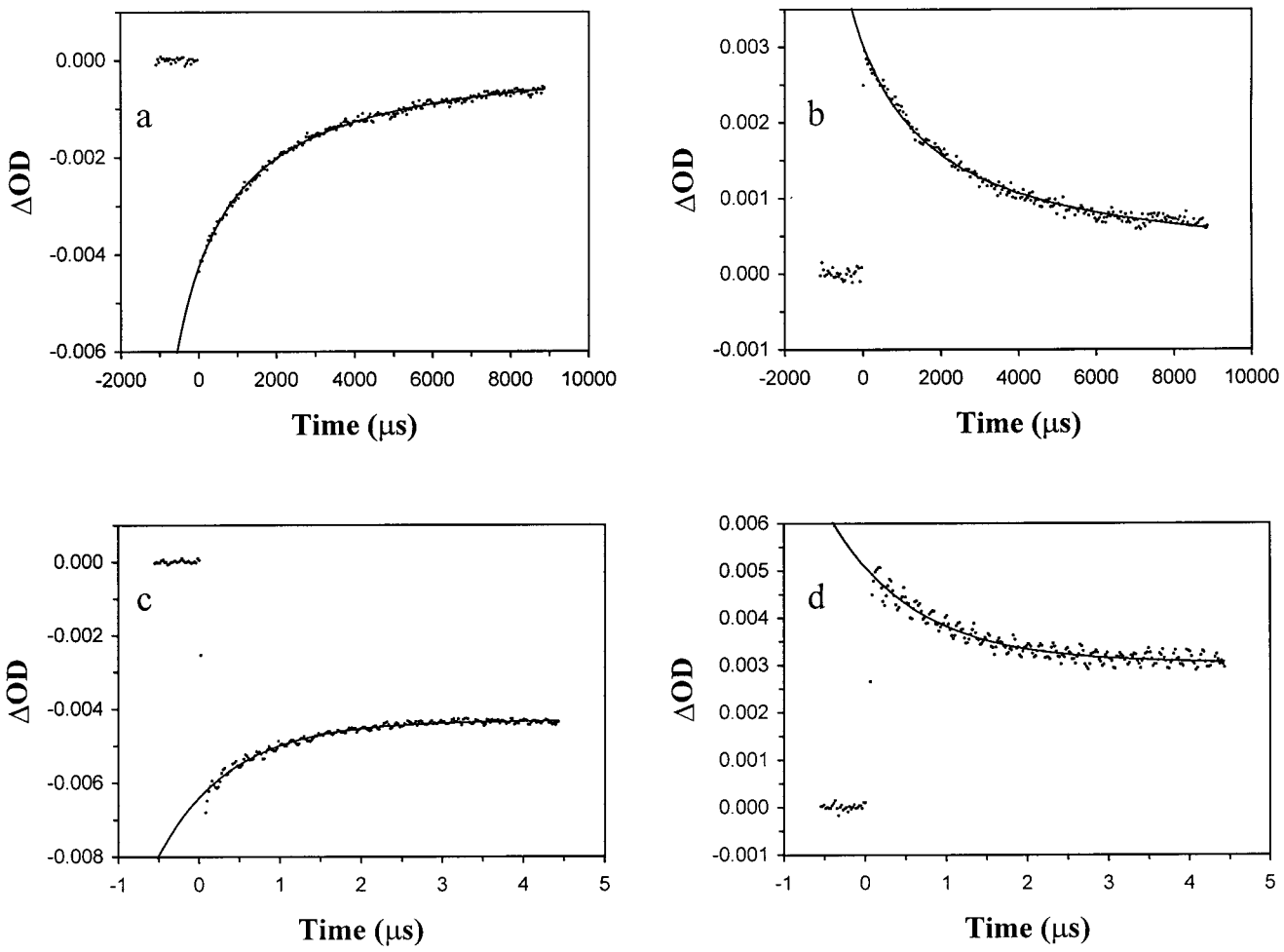

Figure 5. Transient UV−Vis curves detected at different time scales at the characteristic wavelengths of the Cor dianion (512 nm, curves (a) and (c)) and Cor radical anion (659 nm, curves (b) and (d)).

one is identical to the known radical anion spectrum[10] and is almost constant throughout the time range measured (1.2 μs and even longer). The second one is a singlet that is attributed to the photoelectron.[13] Subtraction of the spectrum taken at the last time interval (which contained the spectrum of the radical anion only) from the others indeed yielded the isolated spectra of the photoelectron (not shown). Kinetic analysis of the transient decay of peak-intensity of the photoelectron spectrum revealed a pseudo first-order rate constant corresponding to ca. 1×10^6 s^{-1}. The data described above confirm that the light-induced process under investigation corresponds, indeed, to an electron photoejection from the Cor dianion. Reappearance of the original UV−Vis spectrum of Cor^{2-} and disappearance of the EPR signal for $Cor^{\bullet -}$ over time (>1.0 s at 175 K) furthermore shows that the observed dark process is the back electron transfer to the radical anion, which regenerates the dianion.

As the Cor dianion and Cor radical anion exhibit distinct absorbance bands at $\lambda = 512$ nm and $\lambda = 659$ nm, respectively, the electron photoejection is reflected by the bleaching of the ground-state Cor dianion at $\lambda = 512$ nm and the formation of an absorbance band at $\lambda = 659$ nm. The recombination process between the photoejected electron and $Cor^{\bullet -}$ is then identified by following the recovery of the bleached signal at $\lambda = 512$ nm (for Cor^{2-}) and the decay of the $Cor^{\bullet -}$ at $\lambda = 659$ nm. The back reaction is a relatively slow process (about 40 ms at room temperature), and the electron ejection is completely reversible. The bleached absorption at $\lambda = 512$ nm has a ΔOD value of only ca. 1% of the OD value of the bulk solution at this wavelength. Hence, 256 scans (for each wavelength) using the PMT detector and 1024 scans using the ICCD are needed to be averaged in order to obtain transients with reasonable signal-to-noise ratios. This implies that only a small fraction of the excited dianion population undergoes light-induced electron ejection.

Figure 5 shows the transients corresponding to the recovery of the bleached Cor^{2-}, curve (a), and the decay of $Cor^{\bullet -}$, curve (b). Close inspection of the transients reveals that both transients include components exhibiting a fast recovery of the bleached species, and a fast decay of the radical anion (curves (c) and (d) respectively), followed by slow decaying processes. The fast transients shown in Figure 5(c) and 5(d) followed a first-order rate law, showing similar rate constant values, 1.12×10^6 s^{-1} and 0.97×10^6 s^{-1}, respectively. The transients shown in Figure 5(a) and Figure 5(b) were analyzed for second-order decay fits. The values of the molar extinction coefficients obtained for the respective anionic species were used to calculate the second-order rate constants. The rate constant values obtained for the recovery of the bleached ground-state Cor dianion and the decay of the radical anion are similar, 1.31×10^9 M^{-1} s^{-1} and 0.97×10^9 M^{-1} s^{-1}, respectively. We think, however, that the value calculated for the recombination rate constant based on the dianion regeneration is more accurate than that obtained by the analysis of the radical anion decay, since the absorbance of the radical anion at $\lambda = 512$ nm is negligible, whereas the contribution of the dianion to the total absorption at $\lambda = 659$

nm is significant. Therefore we determine that according to our measurements the back reaction occurs at a rate of $1.3(\pm 0.3) \times 10^9\ M^{-1}\ s^{-1}$. The back electron transfer rate constant of $Cor^{\bullet -}$ and the electron is in agreement with the recombination rates of other polycyclic radical anions with electrons.[1] On the other hand this recombination rate constant is ca. 10-fold slower than the recombination rate constant observed for neutral species and electrons (generated by photoejection of an electron from a radical anion).[3,5,6] The retardation of the back electron transfer with $Cor^{\bullet -}$ is attributed to electrostatic repulsion between the recombining species.

Upon calculating an approximate value for the diffusion rate constant in THF at room-temperature based on viscosity measurements (0.0048 Poise)[3] one obtains a value of $1.4 \times 10^{10}\ M^{-1}\ s^{-1}$, a value that is of 1 order of magnitude higher than the observed rate constant. Thus, the second-order back electron transfer process is not diffusion controlled. The slow rate might originate, as suggested before, from the electrostatic repulsion between the radical anion and the electron. A further contribution to the slow back electron transfer could be the fact that the generated Cor^{2-} exhibits antiaromatic properties whereas $Cor^{\bullet -}$ is nonaromatic around the rim.

The analysis of the kinetic decay of the photoejected electron using EPR spectroscopy, and the transient decay of the Cor radical anion, using laser flash photolysis, reveal important differences. While the photoejected free electron decays within 1 μs in the EPR spectrum at low temperatures, the decay of the Cor radical anion, and the regeneration of the Cor dianion, proceeds on a time scale of several milliseconds! To understand this difference, we examined the initial, primary decay of the $Cor^{\bullet -}$ (and the recovery of the Cor^{2-}) on a short time scale (5 μs), Figure 5(c) and (d). We observe a fast-decaying transient component on a short time scale for the decay of $Cor^{\bullet -}$ (as well as a fast recovery component for Cor^{2-}). Both of these rapid kinetic processes follow first-order kinetics, $k \approx 1 \times 10^6\ s^{-1}$. Following these results, the reactions outlined in eqs 1−5 are formulated to account for the light-induced photoejection of the electron from Cor dianion and the recombination process of the photoejected electron:

$$Cor^{2-} \xrightarrow{h\nu} [Cor^{\bullet -} + e^-]\ \text{(Cage of photoproducts)} \quad (1)$$

$$[Cor^{\bullet -} + e^-] \xrightarrow{k_{rec}^1} Cor^{2-} \quad (2)$$

$$[Cor^{\bullet -} + e^-] \xrightarrow{k_s} Cor^{\bullet -} + e^- \quad (3)$$

$$e^- + Li^+ \rightarrow (Li^+, e^-) \quad (4)$$

$$[Li^+, e^-] + Cor^{\bullet -} \xrightarrow{k_{rec}^2} [Cor^{2-}] + Li^+ \quad (5)$$

(i) Photoexcitation of Cor^{2-} results in photoejection of the electron to yield a cage of photoproducts. In-cage recombination of the photoproducts, eq 2, results in the first-order fast decaying process of $Cor^{\bullet -}$ to yield Cor^{2-}, $k_{rec}^1 = 1.1 \times 10^6\ s^{-1}$. (ii) The electrostatic repulsion within the cage retards the recombination and facilitates the dissociation of the cage complex, eq 3. The slow decaying transient of $Cor^{\bullet -}$ is attributed to the cage-separated photoproducts. From the initial amount of $Cor^{\bullet -}$ and the cage-separated yield of $Cor^{\bullet -}$, we estimate the cage escape rate constant to be $k_s = 2.3 \times 10^6\ s^{-1}$. Thus, the dissociation of the cage products effectively competes with the intracage back electron transfer. (iii) The cage-separated electron is scrambled in solution and is electrostatically attracted by lithium cations. This electron-lithium ion pairing process, eq 4, is anticipated[3−5] to be extremely rapid, i.e., $>10^{12}\ M^{-1}\ s^{-1}$. Association of the electron with the Li^+ ions defies the distinct electronic state of the free electron, and hence the $[Li^+, e^-]$ complex species lacks an EPR signal.[15] Thus, the free electron can only be detected in the cage of photoproducts, and its decay within ca. 1 μs is consistent with the lifetime of the cage structure. (iv) The $[Li^+, e^-]$ ion pair is capable of reducing $Cor^{\bullet -}$, eq 5. The reduction potential of the ion pair is, however, substantially lower,[3−5] resulting in a slow recombination rate, $k_{rec}^2 = 1.3 \times 10^9\ M^{-1}\ s^{-1}$. This slow back electron transfer may be further explained by aromaticity considerations.

Conclusions

We have demonstrated the light-induced ejection of an electron from corannulene dianion and have characterized the photoproducts by means of time-resolved EPR and laser flash photolysis. Electrostatic repulsion between corannulene radical anion and the ejected electron facilitates the dissociation of the initially formed cage of the photoproducts. The formation of a $[Li^+, e^-]$ ion pair after separation of the electron from the radical anion provides a low-energy Li^+-mediated path to overcome electrostatic repulsion between $Cor^{\bullet -}$ and the ejected electron, which facilitates the radical anion/electron recombination process.

Acknowledgment. Financial support from the US-Israel Binational Science Foundation (BSF) and from the U.S. Department of Energy is gratefully acknowledged. R.S. would like to thank Shelly Tzlil and Amit Lerner for assistance in the molar absorption coefficient measurements, Yehuda Heimlich and Prof. Haim Levanon for the EPR experiments, and Julian Wasserman for his invaluable assistance with the UV-Vis flash photolysis system.

References and Notes

(1) Eloranta, J.; Linschitz, H. *J. Chem. Phys.* **1963**, *38*, 2214.
(2) Giling, L. J.; Kloosterboer, J. G.; Rettschnick, R. P. H.; van Voorst, J. D. W. *Chem. Phys. Lett.* **1971**, *8*, 457.
(3) Rämme, G.; Fisher, M.; Claesson, M.; Szwarc, M. *Pro. R. Soc. Lond. A.* **1972**, *327*, 467.
(4) Giling, L. J.; Kloosterboer, J. G. *Chem. Phys. Lett.* **1973**, *21*, 127.
(5) Szwarc. M.; Levin, G. *J. Photochem.* **1976**, *5*, 119.
(6) Fox, M. A. *Chem. Rev.* **1979**, *79*, 253, and references cited therein.
(7) Soumillion, J. P. *Top. Curr. Chem.* **1993**, *168*, 93, and references cited therein.
(8) Szwarc, M. *J. Polym. Sci. Part A: Polym. Chem.* **1998**, *36*, v-xiii, and references cited therein.
(9) Rozenshtein, V.; Zilber, G.; Rabinovitz, M.; Levanon, H. *J. Am. Chem. Soc.* **1993**, *115*, 5193.
(10) Zilber, G.; Rozenshtein, V.; Cheng, P.-C.; Scott, L. T.; Rabinovitz, M.; Levanon, H. *J. Am. Chem. Soc.* **1995**, *117*, 10 720.
(11) Fox, M. A.; Kabir-ud-Din *J. Phys. Chem.* **1979**, *83*, 1800.
(12) Hoijtink, G. J.; Zandstra, P. J. *Mol. Phys.* **1960**, *3*, 371.
(13) van Voorst, J. D. W.; Hoijtink, G. J *J. Chem. Phys.* **1966**, *45*, 3918.
(14) van Voorst, J. D. W.; Hoijtink, G. J. *J. Chem. Phys.* **1966**, *45*, 3918.
(15) Bockrath, B.; Dorfman, L. M. *J. Phys. Chem.* **1973**, *77*, 1002.
(16) Fisher, M.; Rämme, G.; Claesson, S.; Szwarc, M. *Proc. R. Soc. London A.* **1972**, *327*, 481.
(17) van Willigen, H. *J. Am. Chem. Soc.* **1972**, *94*, 7966.
(18) Ayalon, A.; Rabinovitz, M.; Cheng, P.-C.; Scott, L. T. *Angew. Chem., Int. Ed. Engl.* **1992**, *31*, 1636.
(19) Ayalon, A.; Sygula, A.; Cheng, P.-C.; Rabinovitz, M.; Rabideau, P. W.; Scott, L. T. *Science* **1994**, *265*, 1065.
(20) Baumgarten, M.; Gherghel, L.; Wagner, M.; Weitz, A.; Rabinovitz, M.; Cheng, P.-C.; Scott, L. T. *J. Am. Chem. Soc.* **1995**, *117*, 6254.
(21) Weitz, A.; Rabinovitz, M.; Cheng, P.-C.; Scott, L. T. *Synth. Met.* **1997**, *86*, 2159.
(22) Shabtai, E.; Hoffman, R. E.; Cheng, P.-C.; Bayrd, E.; Preda, D. V.; Scott, L. T.; Rabinovitz, M. *J. Chem. Soc., Perkin Trans. 2* **2000**, 129.
(23) Scott, L. T.; Hashemi, M. M.; Bratcher, M. S. *J. Am. Chem. Soc.* **1992**, *114*, 1920.